processes

MDPI

Article

Hybrid Closed-Loop Control for Flue Gas Oxygen in Municipal Solid Waste Incineration with Firefly and Whale Optimization

Jinxiang Pian [1], Yuchen Yang [1,*], Jian Tang [2] and Jing Hou [1]

[1] School of Electrical and Control Engineering, Shenyang Jianzhu University, Shenyang 110168, China; pianjx@sjzu.edu.cn (J.P.); dqhoujing@sjzu.edu.cn (J.H.)
[2] School of Information Science and Technology, Beijing University of Technology, Beijing 100124, China; freeflytang@bjut.edu.cn
* Correspondence: yyc001201@stu.sjzu.edu.cn; Tel.: +86-15545327879

Abstract

Precise control of flue gas oxygen content is essential for stable and efficient operation in municipal solid waste incineration (MSWI) systems. However, the strong nonlinearity and time-varying characteristics of combustion processes often lead to poor performance of conventional proportional–integral–derivative (PID) and open-loop model-based control schemes. To overcome these limitations, this study proposes a hybrid intelligent closed-loop control framework that integrates the firefly algorithm (FA) and whale optimization algorithm (WOA) for adaptive tuning of control parameters under dynamic operating conditions. The proposed system comprises four coordinated modules—preset, oxygen content prediction, predictive compensation, and feedback compensation—forming an adaptive multi-layer control loop. Experimental validation was performed using real operational data from 2 × 600 t/d MSWI plant. When the operating conditions changed from stable to variable, the proposed method maintained the flue gas oxygen content at 7.78%, with an overshoot of 1.53%, a relative error of –0.094%, and a settling time of 90 s. In comparison, the MPC-based control achieved 7.75%, with an overshoot of 2.10%, relative error of –0.529%, and settling time of 100 s, while the existing plant control method achieved 7.85%, with an overshoot of 2.35%, relative error of 0.835%, and settling time of 180 s. These results indicate that the proposed FA–WOA hybrid control framework effectively improves response speed by 50%, reduces overshoot by 34.9%, and enhances control accuracy by over 80% compared with the conventional method. Moreover, the system eliminates manual adjustment and achieves stable combustion performance under fluctuating conditions, demonstrating its potential for intelligent oxygen control and automation in large-scale MSWI plants.

Keywords: hybrid intelligent closed-loop control; feedforward compensator; feedback restoration; flue gas oxygen; waste incineration process

check for updates

Academic Editor: Fabrizio Scala

Received: 22 September 2025
Revised: 26 October 2025
Accepted: 28 October 2025
Published: 3 November 2025

Citation: Pian, J.; Yang, Y.; Tang, J.; Hou, J. Hybrid Closed-Loop Control for Flue Gas Oxygen in Municipal Solid Waste Incineration with Firefly and Whale Optimization. *Processes* **2025**, *13*, 3528. https://doi.org/10.3390/pr13113528

Copyright: © 2025 by the authors. Licensee MDPI, Basel, Switzerland. This article is an open access article distributed under the terms and conditions of the Creative Commons Attribution (CC BY) license (https://creativecommons.org/licenses/by/4.0/).

1. Introduction

With the advancement of urbanization in China, municipal waste incineration for power generation has become a crucial component in waste disposal and energy application. Finding ways to improve the combustion efficiency of waste incineration and reduce combustion costs has become a research focus for many scholars [1]. Flue gas oxygen content is a key technical parameter for determining the combustion efficiency of solid waste. Excessively high or low oxygen content will affect the composition of the finally emitted

gas, thereby influencing the safety of the entire combustion process. Waste incineration is a complex heat transfer and phase change process involving multiple technologies and stages, characterized by strong nonlinearity, time-variability, and variable operating conditions. It is difficult to describe with an accurate mathematical model [2,3]. Therefore, researching effective control technologies for flue gas oxygen content in the municipal solid waste incineration process is an urgent need for the actual operation of municipal solid waste incineration plants.

During the waste incineration process, changes in waste characteristics (such as calorific value and composition) may cause measurable and unmeasurable disturbances [4], affecting the stable control of flue gas oxygen content [5]. Thus, when the incineration process is affected by both measurable and unmeasurable disturbances—especially when operating conditions change—effectively controlling flue gas oxygen content has become an important scientific challenge [6]. Conventional PID control is still widely used in many industrial processes due to its simple structure and easy implementation [7]. However, PID control performs poorly in handling strong nonlinearity, large time delays, and large disturbances [8]. Especially when facing complex system disturbances, PID control cannot effectively distinguish between measurable and unmeasurable disturbances, nor can it systematically handle these disturbances, making it unable to fully adapt to dynamically changing environments [9]. To address this issue, fuzzy control, as a nonlinear control method, handles complex control problems through fuzzy rules. For example, the genetic fuzzy control method optimized by genetic algorithms for fuzzy rules proposed in Reference [10] significantly improved the tracking effect of furnace temperature control; Reference [11] enhanced the stability of the control system by introducing adaptive factors into fuzzy control rules; the fuzzy self-organizing control method proposed in Reference [12] achieved precise control of key process parameters (e.g., furnace temperature and flue gas oxygen content) by optimizing fuzzy rules. Although fuzzy control performs well in handling uncertainty and fuzziness, it still has shortcomings such as its inability to model accurately and adjust precisely [10]. Therefore, fuzzy control often fails to achieve the expected effect when dealing with the control of complex incineration processes with coexisting multiple disturbances [13].

In contrast, model predictive control (MPC) exhibits outstanding performance in handling multivariable coupling, system constraints, and dynamic optimization [14]. For instance, Reference [15] verified through actual data from a municipal solid waste incineration plant that the MPC method can effectively control the main steam flow and flue gas oxygen content. However, MPC usually relies on linearized state-space models, and these assumptions differ greatly from actual industrial processes, resulting in unsatisfactory control effects. Although MPC can provide precise strategies for multivariable control, its handling of disturbances still depends on model accuracy, leading to limitations when facing unmeasurable disturbances [16,17].

In the application of solid waste incineration control technologies, there are significant differences in operating conditions between developed and developing countries [8]. Developed countries usually have advanced technical equipment and control systems and can rely on sophisticated mathematical models and efficient control algorithms (e.g., MPC) to stably maintain the incineration process and ensure the stability of flue gas oxygen content [18,19]. The control systems in these countries are usually mature and efficient, capable of coping with disturbances and optimizing operations well. However, the solid waste incineration process in developing countries often faces greater volatility, and the equipment and technology are relatively backward. The direct application of advanced control methods from developed countries often fails to achieve ideal effects [20,21]. Therefore, after recognizing the limitations of existing control methods, the introduction of

swarm intelligence algorithms has provided new ideas for the control of flue gas oxygen content [22–24]. For example, algorithms such as particle swarm optimization (PSO) and ant colony optimization (ACO) can adaptively adjust control strategies and optimize system parameters by simulating the principles of group behavior in nature [25,26]. Reference [27] points out that swarm intelligence algorithms can not only effectively improve model accuracy but also find the optimal control scheme without relying on an accurate mathematical model. However, due to the complexity and cumbersomeness of the optimization process, these methods often struggle to meet real-time requirements. Adaptive control and hybrid control strategies constitute another research focus at present. Adaptive control systems can automatically adjust control parameters according to changes in system state, thereby avoiding the incompatibility of static control strategies when facing environmental changes [23]. In contrast, hybrid control methods, by combining multiple control strategies and considering the advantages of each method, provide more robust control performance in complex and uncertain environments [28].

Thus, this study combines modeling and control technologies and proposes a hybrid intelligent closed-loop control method integrating feedforward and feedback mechanisms. First, a manipulated variable preset model is established based on the target flue gas oxygen content to provide a benchmark for control operations. The feedforward compensation model uses measurable disturbance information to predictively correct the primary and secondary air volumes based on the manipulated variable benchmark, thereby maintaining the symmetric stability of the system before disturbances are fully manifested. The feedback compensation mechanism, targeting unmeasurable or uncertain disturbances, implements real-time dynamic adjustments based on the deviation between the actual flue gas oxygen content and the target value. Experimental results based on actual operating data show that this method can ensure that flue gas oxygen content is stably maintained near the target value under both measurable and unmeasurable disturbance conditions, effectively realizing an efficient control of flue gas oxygen content during the incineration process.

The major contributions of this paper are as follows:

(1) A novel hybrid control framework combining firefly algorithm (FA) and whale optimization algorithm (WOA) for intelligent, real-time optimization of flue gas oxygen content in MSWI systems.
(2) A closed-loop control structure that integrates predictive compensation and feedback compensation, ensuring continuous adaptation to operational changes without the need for manual intervention.
(3) Real-world validation using operational data from a 600 t/d MSWI plant, demonstrating the method's robustness, accuracy, and scalability for large-scale waste-to-energy plants.
(4) A significant improvement in control performance: a 34.9% reduction in overshoot, 50% faster response time, and over 80% enhancement in control accuracy compared to traditional methods.

These results highlight the practical value and scalability of the proposed hybrid intelligent control system, paving the way for more efficient, autonomous, and adaptable control solutions in MSWI systems and other complex industrial processes.

2. Problem Formulation

2.1. Description of the Waste Incineration Process

A typical solid waste incineration system is illustrated in Figure 1. Municipal waste collected from various urban areas undergoes fermentation and dehydration before being fed into the incinerator. It sequentially passes through the drying grate, combustion grate-1, combustion grate-2, and burnout grate for drying and combustion. Combustion

air required during the combustion stage is injected from below the grate and the middle of the furnace by primary and secondary fans, respectively. High-temperature flue gas in the furnace is drawn into the boiler system, cooled, purified, and then discharged through the chimney. An oxygen content sensor is installed at the tail of the flue gas emission path. The completeness of the incineration process is evaluated by measuring the flue gas oxygen content at the exhaust port. In actual control operations, operators adjust the combustion state by regulating primary and secondary air volumes, maintaining the flue gas oxygen content near the target value.

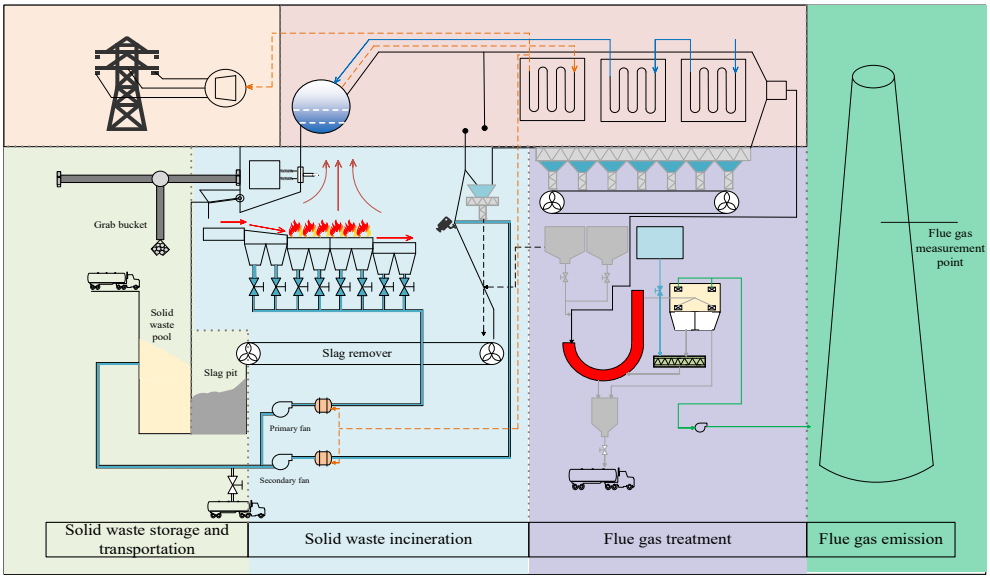


Figure 1. MSWI process flowchart.

2.2. Flue Gas Oxygen Content Control Model

The municipal solid waste incineration process involves a series of complex reactions, including physical and chemical combustion reactions. Oxygen consumption during this process can be described through a material balance. Assuming that the organic matter in the waste is completely burned, the basic combustion reactions are as follows:

$$C_xH_y + (x + \frac{y}{4})O_2 \rightarrow xCO_2 + \frac{y}{2}H_2O \quad (1)$$

Here, C_xH_y is the organic matter in the garbage, O_2 is the oxygen, and CO_2 and H_2O are the products. In this reaction, the oxygen consumption is related to factors such as the carbon–hydrogen ratio of organic matter, the calorific value of waste, and temperature. Through the material balance equation, the oxygen demand can be expressed as

$$\dot{m}_{O_2} = \dot{m}_{fuel} \cdot \frac{a}{M_{fuel}} \quad (2)$$

Here, $\dot{m}_{O_2}$ represents the mass flow rate of oxygen consumed per unit time, $\dot{m}_{fuel}$ represents the mass flow rate of garbage entering the furnace within a unit of time, a is the stoichiometric number of the fuel (the molar ratio of oxygen to organic matter), and M_{fuel} represents the molecular weight of the fuel. The supply of oxygen in the furnace can be adjusted through material balance and oxygen consumption to ensure the completeness of the reaction.

It can be seen that the flue gas oxygen content is related to the oxygen content in the reaction process. The oxygen content, in turn, is associated with the primary air flow rate, secondary air flow rate, feeding rate, and grate speed. The specific analysis is as follows:

Primary air flow refers to the air entering from the bottom of the furnace, which mainly provides oxygen for combustion and plays a key role in combustion adequacy. Appropriate increase can improve oxygen concentration and combustion efficiency, but excessive flow will cause peroxidating, unstable combustion, excessively high flue gas oxygen content, and exacerbate temperature fluctuations and pollutant generation. Secondary air flow is supplied from the upper part or side of the furnace, used to optimize air distribution, promote combustion, and regulate furnace temperature. Suitable flow helps balance air flow and ensure sufficient combustion; excessive flow may cause air disturbance and incomplete combustion, while insufficient flow tends to lead to local overheating and reduced combustion efficiency. Feeding rate determines the amount of solid waste entering the furnace, affecting oxygen demand. When the rate accelerates, insufficient oxygen supply will reduce oxygen content and easily generate harmful gases; an overly slow rate will cause oxygen surplus and energy waste. Its influence presents nonlinear characteristics. Grate speed affects the residence time of waste: excessively fast speed results in incomplete combustion, oxygen waste, and increased pollutants; overly slow speed tends to cause over-combustion and increase pollutant emissions. Its impact on oxygen content is also nonlinear.

In summary, flue gas oxygen content is affected by the primary air flow rate, secondary air flow rate, feeding rate, and grate speed. Among these factors, the feeding rate and grate speed are not suitable for frequent adjustment in practical operations. Moreover, they tend to cause system instability under certain operating conditions. Therefore, in this study, they are regarded as operating conditions rather than direct adjustment objects. Specifically, the feeding rate and grate speed determine the amount of waste entering the furnace chamber and the combustion rate. They can characterize changes in operating conditions, such as waste calorific value, which affects combustion efficiency and stability, and thereby influence the selection of the primary air volume and secondary air volume that need to be adjusted. Thus, the input–output relationship between flue gas oxygen content and its influencing factors can be described by Figure 2. The inputs include the primary air flow rate (u_1), secondary air flow rate (u_2), feeding rate (Ω_1), and grate speed (Ω_2), while the output is the flue gas oxygen content. Here, f() represents an unknown nonlinear relationship. And it can also be expressed by Formula (3).

$$y(t) = f(u_1(i), u_2(i), \Omega_1(i), \Omega_2(i)) \tag{3}$$

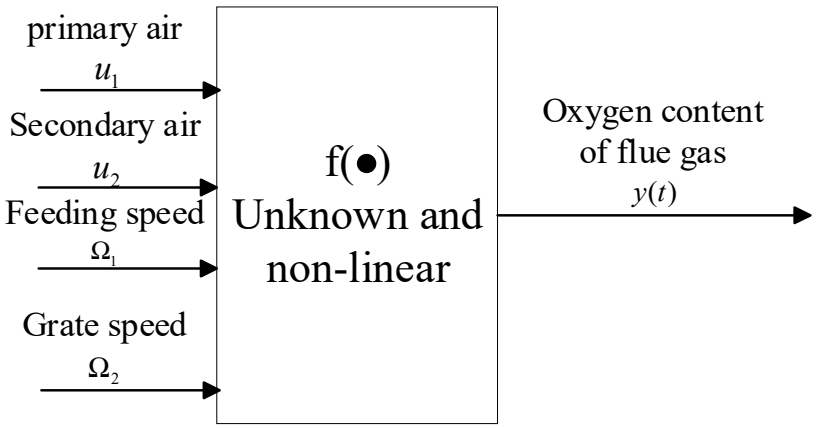


Figure 2. Diagram of the relationship between operating variables and the oxygen content in the output flue gas.

In Formula (3): $y(t)$ represents the oxygen content in the flue gas; F represents a nonlinear relationship; i represents the sampling moment; u_1, u_2 represents the influencing

factors such as primary air volume and secondary air volume; Ω_2 represents working conditions such as feeding speed and grate speed. Therefore, the focus of this study is on the dynamic adjustment method of primary and secondary air volumes. Based on the current operating conditions and potential disturbances, a reasonable adjustment strategy is designed considering these nonlinear relationships to ensure that flue gas oxygen content is controlled within the target range.

2.3. Formal Definition of Steady for Oxygen Content Control

In control theory, for the oxygen content control loop, this equilibrium is defined by its target value [29]. Let $y(t)$ denote the measured oxygen content and O^* denotes its target value. Given the practical requirements of the combustion process, it is neither necessary nor feasible to maintain $y(t) = O^*$ precisely at every moment [30,31]. Instead, the control's objective is to confine y(t) within an allowable interval steady at O^*. The allowable interval S is defined as

$$S = \{y \in R | \, |y - O^*| \leq \varepsilon\} = [O^* - \varepsilon, O^* + \varepsilon] \tag{4}$$

where $\varepsilon > 0$ is the maximum tolerated deviation, determined by process requirements. The system is said to be in a steady state at time t if $y(t) \in S$. Conversely, a steady-breaking event occurs if $y(t) \notin S$.

The disturbances, both measurable and unmeasurable, are the sources of steady breaking [32,33]. The goal of the proposed hybrid intelligent closed-loop control is twofold:

(1) Steady-Preserving: Proactively counteract measurable disturbances through feedforward compensation to prevent $y(t)$ from leaving S.
(2) Steady-Restoring: Reactively eliminate the deviation through feedback compensation to drive $y(t)$ back into S swiftly and smoothly whenever a steady-breaking event occurs.

To illustrate this problem, the parameters are first defined. The controlled variable (CV) is the flue gas oxygen content $y(t)$ with a unit of %. The target value of flue gas oxygen content O^*, assumed to be 6%, serves as the center of steady state. The allowable stable interval S = [5–7%], i.e., $\varepsilon = 1\%$. The manipulated variables (MV) are the primary air volume u_1 and secondary air volume u_2. The main disturbance is the waste Lower Heating Value (LHV) $d(t)$ with a unit of MJ/kg. An increase in LHV leads to higher oxygen consumption, thereby reducing the flue gas oxygen content. Therefore, the gain K_d of this disturbance channel is negative.

The transfer function for the process is defined, where the process channel is

$$G_p(s) = \frac{0.8}{30s + 1} e^{-10s} \tag{5}$$

The disturbance channel is

$$G_d(s) = \frac{-0.5}{25s + 1} e^{-5s} \tag{6}$$

The ideal stable state of the system is defined as the state where the output stabilizes at the target value O^* when all inputs remain unchanged and there is no disturbance. That is, there exists a state xs and a control quantity Us such that

$$\begin{aligned} 0 &= Ax_s(t) + Bu_s(t) \\ O^* &= Cx_s(t) \end{aligned} \tag{7}$$

At this point, the system is in a static stable state.

From the perspective of steady-state impact, if at time t = 50 s, a step disturbance of the increase in the calorific value of garbage by +3 MJ/kg occurs, that is $d(t) = 3\sigma(t-50)$, the disturbance d(t) will disrupt the above equilibrium. According to the model, a stepwise increase in calorific value +3 MJ/kg will cause a steady-state deviation in oxygen content $|K_d \cdot \Delta LHV| = 1.5\% > \varepsilon = 1\%$. Then the system will not be able to return to the original stable interval, $S = [5\%, 7\%]$, automatically but will operate at a new instability equilibrium point $O^* + K_d \cdot \Delta LHV = 4.5\%$. This is a thorough and continuous disruption of the steady state. From the perspective of dynamic impact analysis, at the moment when the disturbance occurs, the rate of decline in oxygen content is determined by the time constant τ_d. The smaller the value of τ_d, the faster the decline and the greater the impact. It is assumed that the dynamic minimum point $y_{\min} = 4\%$ is lower than the final steady-state value of 4.5%. This indicates steady breaking during the dynamic process, which is more severe than the 1.5% steady-state breaking. As a result, the system may stay outside the stable interval S for a longer time. In summary, whether analyzed from a steady-state or dynamic perspective, the waste LHV disturbance exerts a non-negligible impact on the system output. It not only changes the equilibrium point of the system but also causes more severe dynamic deviations during the transient process. Therefore, designing a control method that can offset the disturbance's impact on the steady state and suppress its dynamic process is the key to restoring and maintaining system stability. Against this background, this study proposes a hybrid intelligent closed-loop control method integrating feedforward and feedback mechanisms. It aims to effectively suppress stable disturbances through a cooperative control strategy, ensuring that the flue gas oxygen content remains in a stable state at all times.

3. Design of the Hybrid Intelligent Closed-Loop Control Method

3.1. Control Strategy

This study proposes a hybrid intelligent closed-loop control method as shown in Figure 3. It consists of four parts: a flue gas oxygen content prediction module [34], a preset module, a predictive compensation module, and a feedback compensation module. Among them, the flue gas oxygen content prediction model adopts the IWOA-XGBoost method to calculate the predicted value of flue gas oxygen content $\hat{y}(t)$ based on manipulated variables and operating conditions (feeding rate, grate speed). The operating parameter preset module uses the IFA method to provide the reference points U_0 for primary and secondary air flow rates according to the current operating conditions and target flue gas oxygen content. The feedforward compensator employs the IFA-PI iterative method. It determines the predictive compensation values of primary and secondary air flow rates $U_f(t)$ based on the predictive deviation in flue gas oxygen content $e_f(t)$, where $e_f(t)$ is the difference between the target flue gas oxygen content O^* and the predicted value of flue gas oxygen content $\hat{y}(t)$. The feedback compensator determines the feedback compensation values of the primary and secondary air flow rates $U_b(t)$ based on the deviation in the measured oxygen content in the flue gas $e_b(t)$ by using the IFA-PI iterative method. Where $e_b(t)$ is the difference between O^* and the measured oxygen content of the flue gas $y(t)$, and the total operating variable is $U(t) = U_0 + U_f(t) + U_b(t)$.

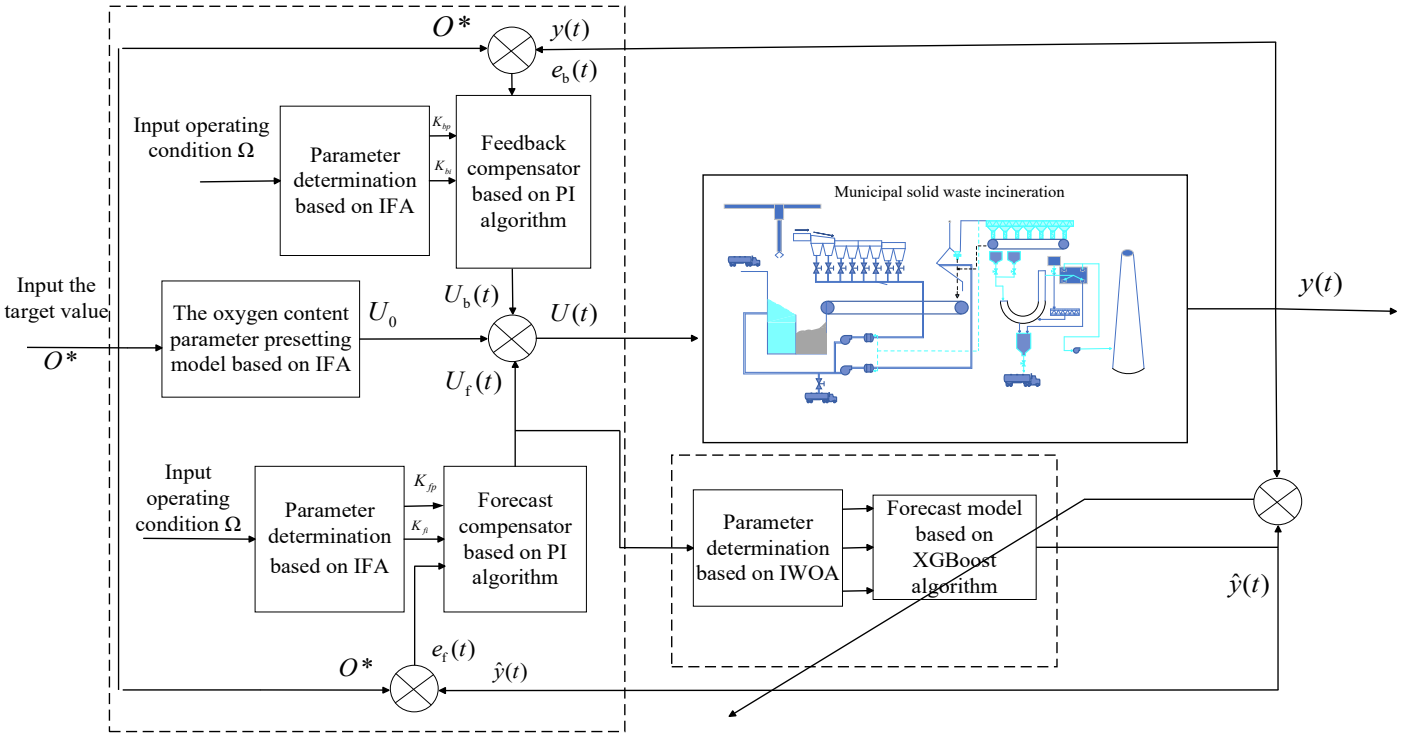


Figure 3. Hybrid intelligent closed-loop control method.

3.2. Control Algorithm

3.2.1. Prediction Model of Oxygen Content in Flue Gas

As shown in Figure 4, the prediction model based on IWOA-XGBoost proposed in this paper consists of two modules: an XGBoost-based flue gas oxygen content prediction module [35] and an IWOA-based parameter optimization module [36]. For the XGBoost-based flue gas oxygen content prediction module, its inputs include primary air flow rate u_1, secondary air flow rate u_2, feed rate Ω_1, and grate speed Ω_2, while its output is the predicted value of flue gas oxygen content $\hat{y}(t)$. The IWOA-based parameter optimization module adopts the IWOA to optimize and determine key parameters in the network model, such as the maximum depth of decision trees D, learning rate λ, and regularization coefficient φ.

(1) The structure of the flue gas oxygen content prediction model based on XGBoost

The output of the XGBoost-based flue gas oxygen content prediction module can be expressed as the sum of results from K trees, as shown in the following formula:

$$\hat{y}(t) = \sum_{k=1}^{K} f_k(x_1) + f_k(x_2), f_k \in F \tag{8}$$

where f_k represents the function of the k-th tree, and F denotes the space of trees. x_1 is the primary air flow rate, x_2 is the secondary air flow rate, and $\hat{y}(t)$ is the output, which refers to the predicted value of flue gas oxygen content.

To balance the accuracy of the flue gas oxygen content model and prevent overfitting, the objective function of XGBoost consists of two components: a loss function and a regularization term that controls the model complexity, as shown in the following formula:

$$Obj = \sum_{i=1}^{4} (y(t) - \hat{y}(t))^2 + \sum_{k=1}^{K} (\varphi T + \frac{1}{2}\lambda \sum_{j=1}^{T} w_j^2) \tag{9}$$

where T is the number of leaf nodes, w_j represents the leaf weights, and φ and λ are the hyperparameters. The number of leaf nodes T is indirectly controlled by limiting tree growth. The hyperparameters involved include maximum depth of the decision tree D—a greater depth leads to a more complex tree with potentially more leaf nodes; and regularization coefficient φ, which is used to penalize leaf weights. A larger regularization coefficient results in a heavier penalty, compressing leaf weight values to become smaller and making the model smoother.

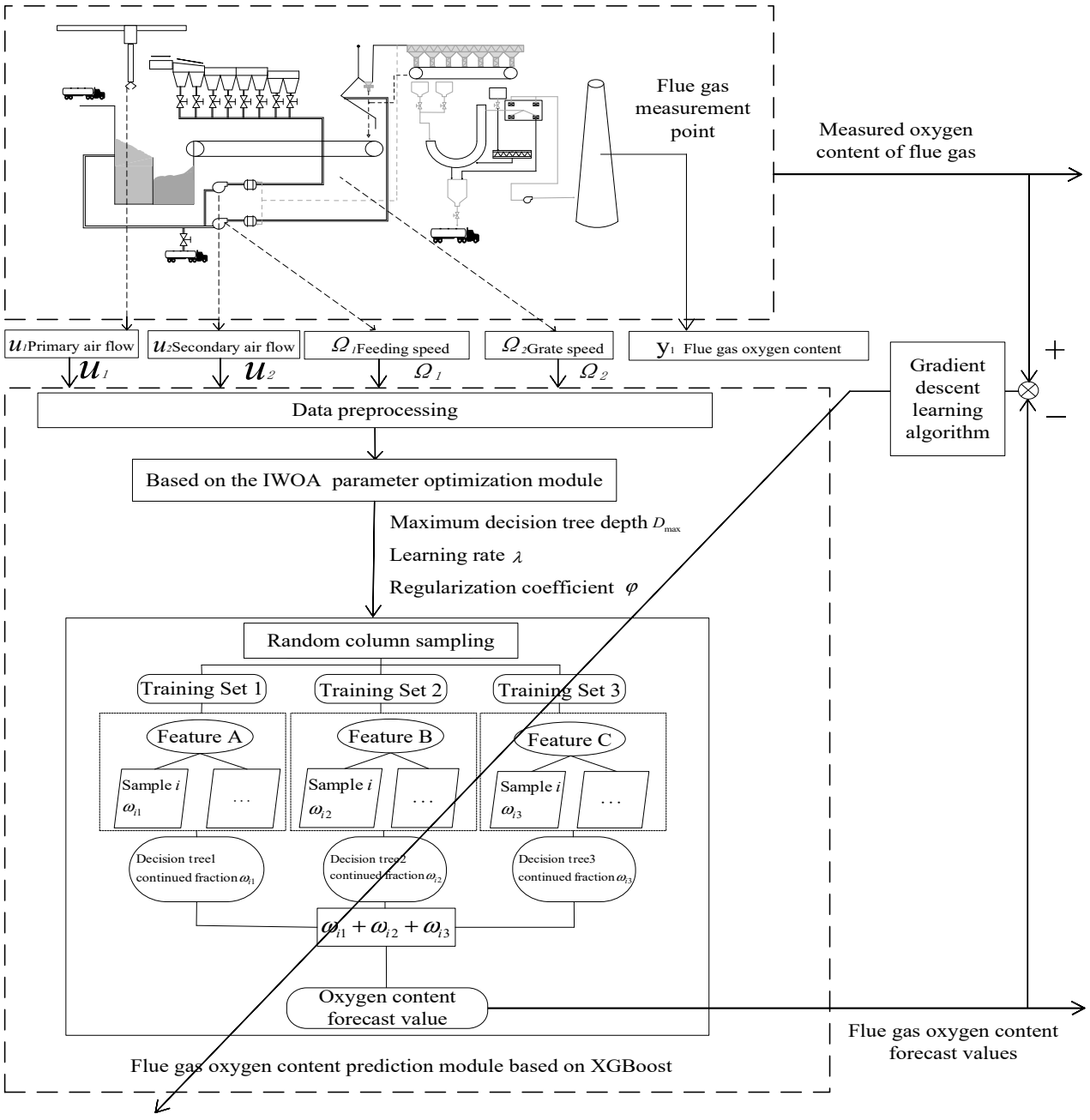


Figure 4. Strategy diagram of the forecast model based on IWOA-XGBoost.

(2) Model parameter determination

As can be seen from the above formulas, the maximum decision tree depth D, learning rate λ, and regularization coefficient φ have a significant impact on model accuracy. In essence, these parameters should be set to different combinations according to varying operating conditions to reflect the characteristics of flue gas oxygen content under different

working conditions. The WOA simulates the hunting behavior of whales through random search, enabling global search. It boasts advantages such as fast search speed and strong global search capability, which allows it to complete the search in a relatively short time while avoiding falling into local optima. By balancing and transforming exploitation and exploration capabilities, the WOA overcomes the limitation that other population optimization algorithms have in local optima, achieving global search optimization. Therefore, this paper first improves the WOA and then uses the improved WOA to optimize the maximum decision tree depth D, learning rate λ, and regularization coefficient φ.

Based on the optimization task, the maximum decision tree depth D, learning rate λ, and regularization coefficient φ are mapped to the whale position vector as follows:

$$X = [\lambda, \overline{D}, \varphi] \tag{10}$$

The parameter range constraints are as follows: $\lambda \in [\lambda_{\min}, \lambda_{\max}]$, $\overline{D} \in [D_{\min}, D_{\max}]$, $\varphi \in [\varphi_{\min}, \varphi_{\max}]$.

The WOA simulates the predation behavior of humpback whales. This algorithm mainly consists of three phases: encircling prey, spiral hunting, and searching for prey.

- Surround the prey

In each iteration of the WOA, the algorithm presets the position of the individual with the optimal fitness in the current population (i.e., the best hyperparameter combination found so far) as the prey's position [37]. Other individuals in the population update their own positions in real time based on this optimal position and the internal variables of the algorithm (A and C). Through this process, these individuals conduct exploration and exploitation around the current optimal solution within the solution space. Its mathematical description is as follows:

$$X(t+1) = X^*(t) - A|CX^*(t) - X(t)| \tag{11}$$

In the formula: t represents the current number of iterations, $X(t)$ represents the position vector of the current search candidate solution, $X^*(t)$ is the position vector of the current optimal search candidate solution, and A and C are coefficient matrices. The calculation formulas for A and C are

$$\left.\begin{array}{l} A = 2ar_1 - a \\ C = 2r_2 \end{array}\right\} \tag{12}$$

In the formula: $r_1 r_2$ is a random vector of [0, 1] and a decreases linearly in [0, 2].

- Bubble nets attack their prey

Humpback whales employ two mechanisms when performing bubble-net attacks: contracting encirclement and spiral position updating. These two types of behaviors occur simultaneously, with humpback whales randomly choosing between shrinking the encirclement or moving along a spiral trajectory. Each method has an equal probability of occurrence (50% each). The position of humpback whales is dynamically adjusted based on the above behaviors, and the corresponding formulas are as follows:

$$\left.\begin{array}{ll} X^*(t) - AD & p < 0.5 \\ X^*(t) + D' e^{bl} \cos(2\pi l) & p \geq 0.5 \end{array}\right\} \tag{13}$$

In the formula: $D' = |X^*(t) - X(t)|$ is the distance between the current search candidate solution and the position of the best search candidate solution; b is the constant that

determines the shape of the spiral path; l is a random number uniformly distributed within $[-1, 1]$; p is a random number within $[0, 1]$.

- Randomly search for prey

Unlike the exploitation phase, in each iteration of this phase, all search candidates except the best one dynamically adjust their positions based on a randomly selected search candidate rather than the current optimal search candidate. The iterative update process is as follows:

$$\left.\begin{array}{l} D = |CX_{rand}(t) - X(t)| \\ X(t+1) = X_{rand}(t) - AD \end{array}\right\} \quad (14)$$

In the formula, $X_{rand}(t)$ is the position vector for randomly searching for candidate solutions.

(3) Improvement in the whale optimization algorithm

In the classic WOA, there exist problems of insufficient convergence accuracy and convergence speed. Meanwhile, although whale individuals can exchange information with each other, they still tend to fall into local optimal solutions. To address the above issues, this paper adopts two improved strategies to optimize the WOA.

- Elite reverse learning strategy

To improve the quality of the initial population, ensure the efficient progress of subsequent iterations of the WOA and avoid problems of slow convergence rate and premature convergence caused by poor initial population quality. The elite opposition-based strategy is introduced into the population initialization stage of the WOA in this study to enhance the overall quality of the initial population. Its core solution steps are as follows:

Suppose $w_i = (w_{i,1}, w_{i,2}, \cdots, w_{i,n})(i = 1, 2, \cdots, n)$ represents an elite individual in a d-dimensional space, then the definition of the corresponding reverse solution $\widetilde{w}_i = (w_{i,1}, w_{i,2}, \cdots, w_{i,d})$ is as follows:

$$\widetilde{w}_{i,j} = rand \times (lb_j + ub_j) - w_{i,j} \quad (15)$$

where $\widetilde{w}_{i,j}$ denotes the j-dimensional vector of the reconstructed solution $\widetilde{w}_i$, $rand$ is a random number of $[0, 1]$, and $lb_j = \min(w_{i,j})$ and $ub_j = \min(w_{i,j})$ are, respectively, the boundaries of the population space. To prevent the elite reverse solution from crossing the boundaries, an out-of-bounds judgment and update are required.

$$\widetilde{w}_{i,j} = \begin{cases} rand \times (ub_j - lb_j) + lb_j & \text{if } \widetilde{w}_{i,j} > ub_j \\ & or\ \widetilde{w}_{i,j} < ub_j \\ \widetilde{w}_{i,j} & else \end{cases} \quad (16)$$

By integrating the elite strategy and the opposition-based strategy, this strategy expands the feasible solution space while retaining high-quality solutions. It effectively improves the spatial diversity and quality of the initial population, providing a high-quality population foundation for the subsequent iterations of the algorithm.

- Nonlinear convergence factor

Analysis of the WOA shows that when $|A| \geq 1$, the population search range tends to expand, and the algorithm is in the exploration stage of the solution space; when $|A| < 1$, the population enters the local exploitation stage, and the search range in this stage is mainly determined by the value of the convergence factor a.

To enhance the global exploration performance of the algorithm in the early and middle stages of iteration, it is necessary to ensure that the convergence factor maintains a relatively high value and shows a slow downward trend in these stages. To achieve this goal,

the inverse cumulative distribution function of the chi-square distribution is introduced in this study to optimize the dynamic characteristics of the convergence factor, thereby improving the parameter a in Equation (19). The corresponding formula is as follows:

$$a = F^{-1}(0.9 - \frac{0.9t}{\max_iteration}|30) \times \frac{2}{F^{-1}(0.9|30)} \tag{17}$$

$$x = F^{-1}(p|v) = \{x : F(x|v) = p\} \tag{18}$$

$$p = F(x|v) = \int_0^x \frac{t^{(v-2)/2} e^{-\frac{t}{2}}}{2^{\frac{v}{2}} \Gamma(\frac{v}{2})} dt \tag{19}$$

In the equations above, p is the probability value, taking values within the range of $[0, 1]$; v is the degree of freedom; $\Gamma(\bullet)$ is the gamma function; t represents the current number of iterations; max_*iteration* represents the maximum number of iterations.

(4) Implementation steps of the flue gas oxygen content prediction model

The specific implementation steps of the IWOA-XGBoost prediction model are as follows:

① Initialize the whale population

A certain number of whale individuals are generated randomly. The position of each whale represents a set of XGBoost model parameters, including maximum decision tree depth, learning rate, and regularization coefficient. During initialization, the value range of parameters is reasonably set according to the actual problem to ensure the algorithm searches within a meaningful search space.

② Calculate the fitness value of each whale

Each set of parameters is substituted into the XGBoost model to predict the training data. The mean square error (MSE) between the predicted values and actual values is calculated as the fitness value. The formula of the fitness function is as follows:

$$MSE = \frac{1}{N} \sum_{n=1}^{N} \left(y(t) - \hat{y}(t)\right)^2 \tag{20}$$

Here, N represents the sample quantity, $y(t)$ represents the actual output, and $\hat{y}(t)$ represents the model output.

③ Identify the current optimal whale

Among all whale individuals, the whale with the smallest fitness value is selected as the current optimal whale (xbest). The position of this whale represents the optimal XGBoost model parameters found so far.

④ Enter the iterative process

Step 1: Calculate parameters A and C based on the adaptively adjusted parameter A.

Step 2: Select different search strategies according to the value of A.

Step 3: Substitute the updated whale position into the XGBoost model and recalculate the fitness value. If the new fitness value is better than the previous one, update the whale's position and fitness value.

Step 4: After all whale individuals are updated, select the whale with the smallest fitness value again as the new optimal whale (xbest).

Step 5: Judge the termination condition. If the termination condition is not met, repeat Step 3 until the condition is satisfied when reaching the maximum number of iterations or the fitness value converges to a certain precision. At this point, the position of the optimal whale is the optimized XGBoost model parameters. The flowchart is shown in Figure 5.

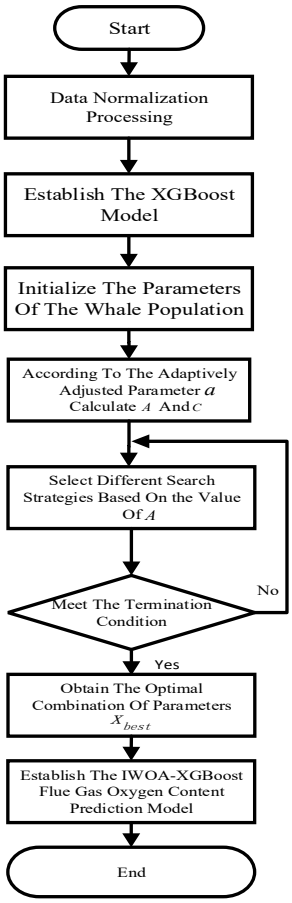


Figure 5. Flowchart of improved whale optimization algorithm.

3.2.2. Presettings for Manipulating Variables

The FA provides a new approach for solving complex problems in dynamic environments [38,39]. In this paper, the FA is used to preset the operation amount of flue gas oxygen content. By simulating the attraction and movement mechanisms of fireflies, the FA can conduct extensive exploration in the search space. The oxygen content optimization problem in the waste incineration process may have multiple local optimal solutions, and the global search capability of the FA can help find a better set value of oxygen content.

Suppose the goal is to find the optimal combination of operating parameters (u_1 primary air flow, u_2 secondary air flow) under specific operating conditions (Ω_1 feeding rate, Ω_2 grate speed) so that the flue gas oxygen content $y(t)$ is as close as possible to the target value O^*. The objective function is defined by the following formula:

$$\min\{f(x)\} = \min\left\{(y_1 - O^*)^2\right\} \tag{21}$$

$$FA_i = [u_1(i), u_2(i), \Omega_1(i), \Omega_2(i)] \tag{22}$$

$$\mu_k^{(i)} \in [\mu_{k,\min}, \mu_{k,\max}], k = 1, 2 \tag{23}$$

$$I_i = \frac{1}{1 + f(u_i)} \tag{24}$$

where FA_i represents the position of each firefly i, indicating a set of parameters. $\mu_k^{(i)}$ represents the range of parameters that need to be constrained. Brightness I_i reflects the

quality of the solution. The formula for the attenuation of the attraction β_{ij} of firefly i to firefly j with distance is

$$\beta_{ij}(r_{ij}) = \beta_0 \times e^{-\gamma \cdot r_{ij}^2} \tag{25}$$

In the formula, β represents the maximum attractive force, β_0 indicates the attractive force of the firefly $(r = 0)$ at the light source, and usually β_0 = 1. γ represents the light intensity absorption coefficient, and its value affects the convergence speed and optimization effect of the FA. γ_{ij} is the Euclidean distance between fireflies, and the formula is

$$r_{ij} = \left\| x_i - x_j \right\| = \sqrt{\sum_{k=1}^{4} \left(x_{i,k} - x_{j,k} \right)^2} \tag{26}$$

For each firefly i, if there exists a brighter firefly j (i.e., $I_j > I_i$), then i moves towards j, and the formula is

$$x_i^{new} = x_i + \beta_{ij} \cdot (x_j - x_i) + \theta \cdot \varepsilon_i \tag{27}$$

where θ is a random step size factor (usually decreasing with iteration), ε_i is a random perturbation vector, and its components are taken from the uniform distribution $[-0.5, 0.5]$.

In the traditional FA, there are problems such as being prone to falling into local optima, along with slight deficiencies in convergence accuracy and convergence speed. To address these issues, this paper adopts three strategies to improve the FA.

- Population initialization based on chaotic optimization strategy

Chaotic motion exhibits characteristics such as randomness, ergodicity, and initial value sensitivity, which can be effectively utilized. In a specific implementation, the variables to be optimized are first mapped to the value range of chaotic variables according to chaotic mapping rules, and then the generated chaotic sequences are converted to the search space of the objective function through linear transformation.

Among various chaotic sequence models, the ergodic performance of sequences generated by the logical self-mapping function is better than that of the traditional Logistic mapping. Therefore, the logical self-mapping function is selected in this study to generate the required chaotic sequences, as shown in Equation (28):

$$y_{(n+1),d} = 1 - 2 * y_{n,d}^2, y_{n,d} \in (-1, 1), n = 0, 1, \cdots \tag{28}$$

Here, to prevent the chaotic sequence from being all 1 or 0.5, the initial values cannot be 0 or 0.5, and d represents the d-th dimension of the D-dimensional search space.

- Evolutionary computation model based on inertia weight

To enhance the local and global search performance of the algorithm, an inertia weight parameter is introduced. Meanwhile, the guiding role of the optimal individual in the population for other individuals is strengthened. The improved position update is given in Equation (29):

$$\begin{aligned} &x_j(t+1) = \omega(t) \times x_j(t) + \beta_{ij}(r_{ij})(x_i(t)) + \\ &a(rand - 1/2) + \omega(t) \times rand \times (x_{best}(t) - x_j(t)) \end{aligned} \tag{29}$$

In the formula, $\omega(t) \times x_j(t)$ represents the influence of a firefly individual's position in the previous iteration on its current position. $\omega(t) \times rand \times (x_{best}(t) - x_j(t))$ denotes the traction effect provided by the optimal individual of the population in the current iteration on other individuals in the population; it is used to control the degree of influence of the current optimal population individual on other individuals as well as the inheritance of the current individual from previous-generation individuals. To make full use of the objective

function information, enhance the guidance of the search direction, and further improve the individual movement speed, a new adaptive inertia weight is proposed. Its calculation formula is shown in Equation (30):

$$\omega(t) = e^{-\left|\frac{1}{(f(x_{best}(t))-M(f))^2+(f_i(t-1)-f_i(t-2))^2}\right|} \tag{30}$$

In the formula, $f(x_{best}(t))$ is the global optimal value at the t-th iteration. $f_i(t-1)$ and $f_i(t-2)$ represent the values of firefly i at the $t-1$-th and $t-2$-th iterations, respectively. $M(f) = \frac{1}{n}\sum_{i=1}^{n} f(x_i(t))$ is the average value of the population objective function at the t-th iteration.

- Population mutation operation based on the Gaussian distribution

A typical manifestation of the population falling into local optima in the FA is the stagnation of the evolutionary process, which is specifically reflected in the fact that the optimal value of the population does not change during multiple consecutive generations of iteration. Based on the experimental results, a judgment criterion is initially set: if the global optimal value of the population still does not change after six consecutive iterations, the algorithm can be determined to have entered an evolutionary stagnation state, i.e., trapped in the region of local optimal solutions.

To help the firefly population break free from the constraints of local optimal values, a Gaussian distribution is introduced in this study to perform mutation processing on the population. Gaussian probability distribution is widely used in the engineering field and plays a positive role in improving the efficiency of engineering optimization designs. The probability density function of the Gaussian distribution is shown in Equation (31).

$$f(x) = \frac{1}{\sqrt{2\pi}\sigma} e^{-\frac{(x-\mu)^2}{2\sigma^2}}, -\infty < x < +\infty \tag{31}$$

Here, σ is the variance of the Gaussian distribution, and μ is the expectation.

All firefly individuals in the population are sorted by the value of the objective function. The top $10\% \times n$ optimal fireflies are used to replace and update the state of the last $10\% \times n$ fireflies in the ranking. Meanwhile, Gaussian mutation is applied to the state of the updated firefly group, and the mutation formula is shown in Equation (32).

$$x_i = x_i \times (1 + N(0,1)) \tag{32}$$

Here, $N(0,1)$ is a random vector, and it follows a Gaussian distribution with a mean of 0 and a variance of 1.

In summary, as shown in Figure 6, based on the standard FA, this study introduces the chaotic optimization strategy, inertia weight, Gaussian mutation, and other components into the FA, and proposes an improved evolutionary model and a chaos-optimized FA for the presetting of flue gas oxygen content. The execution process of this algorithm is described as follows:

Step 1: Parameter initialization according to Equation (28). Initialize parameters, including the number of fireflies, problem dimension, light absorption coefficient, initial value of step factor, maximum attractiveness factor, maximum number of iterations, and search accuracy.

Step 2: Population initialization. Generate initial solutions using chaotic sequences, map them to the solution space of the FA, and determine the positions of the initial population.

Step 3: Fitness evaluation and ranking. Calculate the objective function value (i.e., fluorescence brightness) of each firefly using Equation (24), sort the fireflies by fitness, and record the current optimal solution and its position.

Step 4: Determination of firefly movement direction. Calculate the distance between individuals and relative fluorescence brightness using Equation (25), and compare the brightness of neighboring fireflies to determine the movement direction.

Step 5: Position update. Calculate the individual attractiveness using Equation (26), and update the spatial coordinates of fireflies combined with the dynamic inertia weight adjustment strategy.

Step 6: Population optimization and mutation. Update the step size using Equations (29) and (30), re-evaluate the fitness, and record the optimal solution. If no improvement is achieved after six consecutive iterations, replace the worst individual with the optimal individual and perform Gaussian mutation on the new population.

Step 7: Termination condition judgment. If the accuracy requirement is met or the maximum number of iterations is reached, terminate the algorithm; otherwise, return to Step 3 to continue optimization.

Step 8: Result output. Output the optimal solution and complete the calculation.

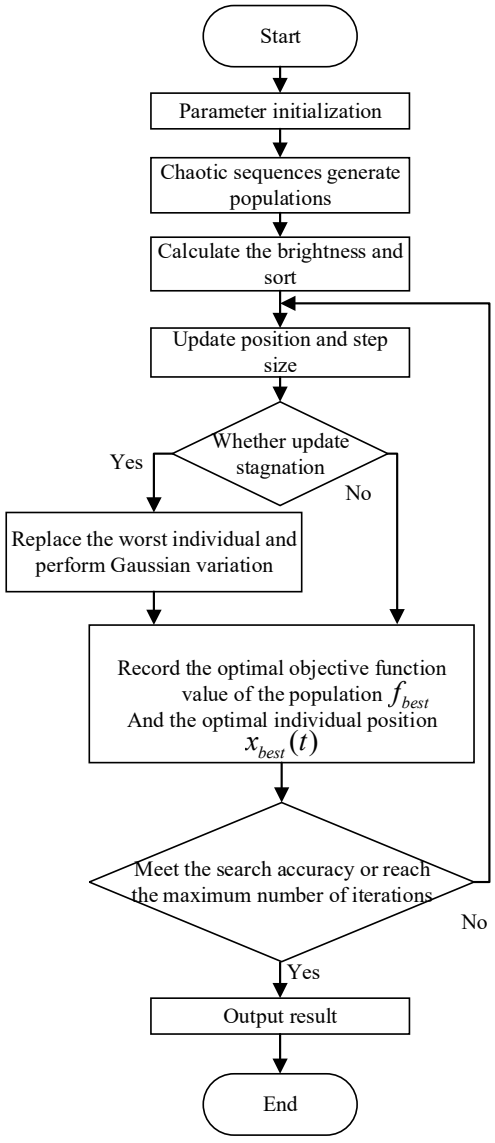


Figure 6. Flowchart of improved firefly optimization algorithm.

3.2.3. Feedforward Compensator and Feedback Compensator

The prediction compensator derives the prediction compensation value of the control variable U_f based on the prediction deviation between the predicted value e_f of the flue gas oxygen content and the target value, so as to control the prediction deviation in the flue gas oxygen content within an allowable range. The specific algorithms are as follows:

$$U_f(n) = K_{\text{fp}} e_f(n) + K_{\text{fi}} \sum_{k=1}^{n} e_f(k) \tag{33}$$

$$e_f(i) = O^* - \hat{O}(i) \tag{34}$$

In the formula, $U_f(n)$ represents the predictive compensation quantity after PI adjustment. The relevant control quantities are adjusted according to the predictive compensation quantity U_f of the control variable. K_{fp} and K_{fi} denote the proportional and integral parameters under the current operating conditions, respectively, which are optimized by the IFA.

Through PI control adjustment, the deviation is kept within a certain range $\left|e_f(n)\right| < \sigma_f$. Based on the current operating conditions (feeding rate and grate speed), the predictive compensation quantities of primary air volume and secondary air volume are obtained.

The feedback compensator adopts the variable PI iterative learning method based on the IFA, as shown in Formula (28). According to the feedback deviation e_b between the measured oxygen content in the flue gas during the solid waste incineration process and the target value, the feedback compensation value U_b of the control variable is obtained.

$$U_b(i) = K_{bP} e_b(i) + K_{bi} \sum_{h=1}^{i} e_b(h) \tag{35}$$

$$e_b(i) = O^* - O_m(i) \tag{36}$$

In the formula, the feedback deviation e_b is the deviation between the measured value O_m(i) of the flue gas oxygen content and the target value O^* of the flue gas oxygen content. The variable U_b(n + 1) represents the feedback compensation value of the manipulated variable after n times of PI iterative learning. Here, K_{bp} and K_{bi} denote the proportional gain and integral time constant, respectively, which are optimized and determined by the IFA according to the current operating conditions (feeder speed, grate speed).

Under the IFA, the optimization task of PI parameters can be analogous to food source searching behavior. In this analogy, the optimal potential values of PI parameters correspond to the positions of food sources, while the firefly population symbolizes the potential solution set of the problem. The exploration and foraging behaviors of fireflies within the search space essentially represent the algorithm's pursuit process for the optimal PI parameters. To achieve a high degree of agreement between the predicted value and target value of the flue gas oxygen content, the feedforward fitness function is set as Equation (37), and the feedback fitness function is set as Equation (38).

$$E_f = \sqrt{\left(O^* - \hat{O}(i)\right)^2} \tag{37}$$

In the formula, $\hat{O}(i)$ is the predicted value of the flue gas oxygen content corresponding to the updated manipulated variables. O^* is the target value of the flue gas oxygen content.

$$E_b = \sqrt{\left(O^* - O_m(i)\right)^2} \tag{38}$$

In the formula, O^* represents the target value of oxygen content in the flue gas; $O_m(i)$ is the measured value of the oxygen content in the flue gas when updating the operation variable.

Table 1 is the IFA optimization algorithm corresponds to the PI parameter optimization problem. The IFA is adopted to optimize and determine the PI parameters, and this process is based on the PI parameter determination module constructed by the IFA. The module compares the predicted value $\hat{O}(i)$ of the flue gas oxygen content with the target value O^* to obtain the prediction deviation e_f. To obtain the PI parameter combination that meets the requirements of current operating conditions, steps such as parameter initialization, initial population evaluation, iterative optimization, and optimal solution output need to be performed.

Table 1. The IFA optimization algorithm corresponds to the PI parameter optimization problem.

Firefly Optimization Behavior	PI parameter Optimization Problem
Firefly swarm	The feasible parameter set of PI
The location of fireflies	PI parameters: proportional coefficient, integral coefficient
The attraction process of fireflies	Search for the optimal solution

3.2.4. Implementation Process of Stable Hybrid Intelligent Closed-Loop Control Method

The flowchart of the hybrid intelligent control method for flue gas oxygen content is shown in Figure 7. In summary, the flue gas oxygen content control combines flue gas oxygen content prediction, flue gas oxygen content presetting, flue gas oxygen content prediction compensator, feedback compensator, IFA, and PI control algorithm. The proposed flue gas oxygen content control can be summarized by the following formula:

$$U_{F_{YF}} = U_0 + U_{bF_{YF}} + U_{fF_{YF}} \tag{39}$$

$$U_{F_{EF}} = U_0 + U_{bF_{EF}} + U_{fF_{EF}} \tag{40}$$

In the formula: $U_{F_{YF}} U_{F_{EF}}$, respectively, represent the air volume of primary air and secondary air. U_0 is the reference set value output by the preset module. $U_{bF_{YF}} U_{bF_{EF}}$ represents its corresponding forecast compensation value. $U_{fF_{YF}} U_{fF_{EF}}$ is its corresponding feedback compensation value. The specific algorithm steps are summarized as follows:

Step 1: Input the target value of flue gas oxygen content and current operating conditions into the preset model. Based on the content in Section 3.2.2, calculate the preset values of the operating variables that can meet the target value of flue gas oxygen content under current operating conditions using the IFA.

Step 2: Input the initial operating variable set values and current operating conditions into the prediction model. Using the content in Section 3.2.1, obtain the initial predicted value of the flue gas oxygen content under current operating conditions through the IWOA-XGBoost-based prediction module.

Step 3: Send the initial operating variable set values to the automatic control system. The automatic control system controls operating variables such as primary air flow and secondary air flow of the municipal solid waste incineration system according to the current operating variable set values, and obtains the measured value of flue gas oxygen content.

Step 4: Compare the initial predicted value of the flue gas oxygen content with the target value. Send the prediction deviation obtained according to Formula (23) to the prediction compensator, and obtain the prediction compensation operation amount through the prediction compensator based on the content in Section 3.2.3.

Step 5: Compare the measured value of the flue gas oxygen content with the target value. Send the feedback deviation obtained according to the feedback compensator, and obtain the feedback compensation operation amount through the feedback compensator.

Step 6: Send the total operating variable value, which is the sum of the initial operating variable set values, feedback compensation operation amount, and prediction compensation operation amount to the prediction model and automatic control system. The predicted value and measured value obtained using the content in Section 3.2.1 are corrected again through the prediction compensator and feedback compensator, and finally a stable total operating variable is obtained.

Step 7: Meanwhile, the predicted value obtained by the prediction model each time is compared with the measured value. The deviation part enables the prediction model to perform self-learning through the gradient descent algorithm, so that the prediction model can find the predicted value more consistent with the measured value within a shorter number of iterations.

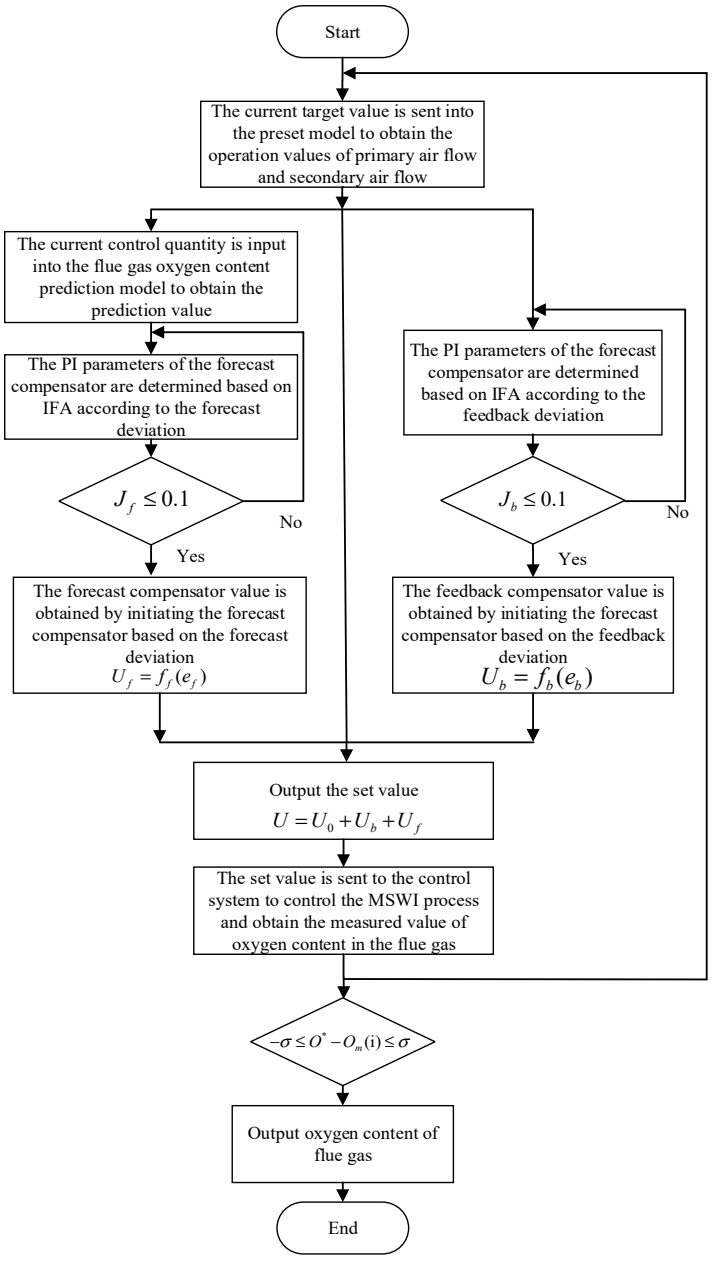


Figure 7. Implementation flowchart of hybrid intelligent closed-loop control.

4. Case Analysis and Experimental Research

4.1. Description of Experimental Data

The operating environment of the experimental platform in this paper is Windows 11, with an AMD (R) RYZEN (TM)-7945HX processor and 16 GB of memory. MATLAB R2021a software is used for programming to realize model training and prediction.

The experimental investigation was conducted at an MSWI plant, located in Beijing, China. This facility is one of the city's key waste-to-energy demonstration projects. The plant has a designed capacity of 2 × 600 t/day of MSW and is equipped with 2 × 12 MW steam turbine generator units. It operates under strict national emission and monitoring standards, providing a stable and representative platform for real-world combustion control research. As shown in Figure 8, the original industrial data used in this experiment were obtained with a 1 s sample period which is equipped with a safety isolation acquisition device. DCSs with closed characteristics are strictly limited in their ability to connect with external devices for data collection and algorithm testing. As a result, we have designed a data acquisition system with a security isolation mechanism, which achieves absolute physical separation between the internal DCS and the external data acquisition system through a unidirectional optical fiber. Data collection was conducted using an edge verification platform at an MSWI power plant.

(1) Data Source and Measurement System

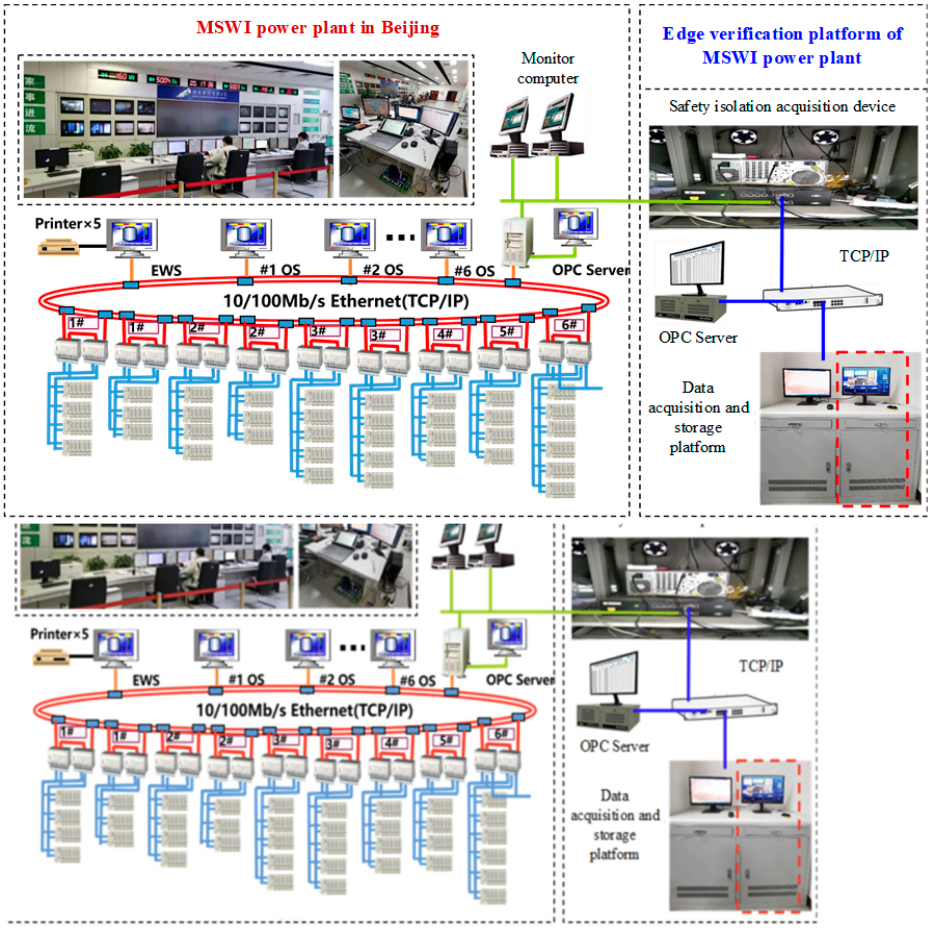


Figure 8. Structure of edge verification platform of MSWI power plant in Beijing.

All operational data used in this study were obtained directly from the plant's Distributed Control System (DCS) during normal incineration operation. The system continuously records key process parameters, including flue gas oxygen content, furnace tem-

perature, and the primary and secondary air flow rates. To ensure measurement precision and repeatability, the following industrial-grade instruments were used and maintained under regular calibration protocols:

① Flue gas oxygen content: zirconia-type oxygen analyzer (accuracy ± 0.1%), as shown in Figure 9.



Figure 9. Zirconia-type oxygen analyzer.

② Air flow: vortex flowmeter (accuracy ± 0.5%), as shown in Figure 10.



Figure 10. Vortex flowmeter.

③ Furnace temperature: K-type thermocouple (accuracy ± 1 °C), as shown in Figure 11.

All sensors and transmitters conform to national metrological standards and are inspected periodically by certified maintenance engineers. The DCS automatically logs operating data at a sampling period of 1 s, providing high-frequency temporal resolution that enables accurate analysis of transient combustion dynamics and control responses.

(2) Data Collection Period and Rationale

The dataset covers 18,000 pieces of historical data from different time periods in September 2022 to Match 2023, as shown in Table 2, which represents a stable operating period with consistent waste feed quality, no scheduled maintenance shutdowns, and no external disturbances. At present, the plant primarily operates under manual intervention mode, leading to highly uniform daily operating conditions. Therefore, selecting this one-month dataset ensures internal consistency and reliability, minimizing the influence of random operational variability. This period was chosen deliberately to provide a clear and controlled environment for evaluating the dynamic performance of the proposed hybrid

intelligent control algorithm. Future research will extend the dataset to multiple months and include different operational modes (e.g., automatic control) to further verify long-term adaptability and robustness.



Figure 11. K-type thermocouple.

Table 2. Operation data collected from a solid waste incineration plant in Beijing.

Sample	Feeder Speed	Grate Speed	Primary Air Volume	Second Air Volume	Oxygen Content in G1 Flue Gas
1	8.63	8.72	0.019,34	0.085,40	6.504,78
2	8.42	8.56	0.019,28	0.112,96	6.587,01
3	8.57	8.34	0.019,16	0.173,60	6.360,22
⋮	⋮	⋮	⋮	⋮	⋮
17,999	9.03	8.77	0.018,55	9.571,27	7.535,53
18,000	9.08	8.57	0.018,49	9.598,88	7.645,50

4.2. Parameter Configuration

Before using the IWOA-XGBoost flue gas oxygen content prediction model for prediction, the parameters of the model need to be set as shown in Table 3. The parameter settings in IWOA include the number of whales: $n = 20$, the search range of whales: -5 to 5, and the maximum number of iterations: $MCN = 1000$. The iterative model of XGBoost is set as *Gbtree*, and the parameters of XGBoost are obtained through optimization using the IWOA. Table 3 also shows the parameters of the flue gas oxygen content prediction model optimized by the IWOA.

Table 3. Parameter configuration of the MSWI flue gas oxygen content prediction model based on IWOA-XGBoost.

Parameter Settings of IWOA		Parameter Settings of XGBoost	
The number of whales	$n = 20$	Iterative model	Gbtree
Search scope	−5~5	The range of gamma values	0~20
Maximum number of iterations	$MCN = 1000$	The range of values for max_depth	3~10

Determination of parameters for the control variable preset model, prediction compensation model, and feedback compensation model of flue gas oxygen content: These parameters refer to those in the performance indicators of the feedback and prediction compensation models. By combining on-site operating conditions with expert experience, the parameters of the IFA are obtained, as listed in Table 4: the search range of fireflies is 0.1–10; the maximum number of iterations is $T = 1000$; the maximum attraction is $\beta = 0.3$; the light intensity absorption coefficient is $\gamma = 0.1$; and the step size factor is $\theta = 0.1$. The parameters of the preset model, feedback, and forecast compensator are optimized by using the IFA.

Table 4. Improve the parameter settings of the firefly optimization algorithm.

Population of Fireflies	The Search Range of Fireflies	Maximum Number of Iterations	Maximum Attraction	Light Intensity Absorption Coefficient	Step Size Factor
20	0.1~10	1000	0.3	0.01	0.5

4.3. Results and Analysis

Figure 12 shows the comparison of the prediction deviation in the proposed flue gas oxygen content prediction model with those of the WOA-XGBoost and PSO-XGBoost models. To further illustrate the superiority of the IWOA-XGBoost model, we can analyze specific data points: When time is around 150 s, the predicted value of PSO-XGBoost drops to about 7.20%, while the measured value is around 7.38%, with a deviation of about 0.18%. The WOA-XGBoost model has a value of about 7.25% at this time, with a deviation of about 0.13%. In contrast, the IWOA-XGBoost model maintains a value close to 7.35%, and the deviation from the measured value (about 7.38%) is only about 0.03%.

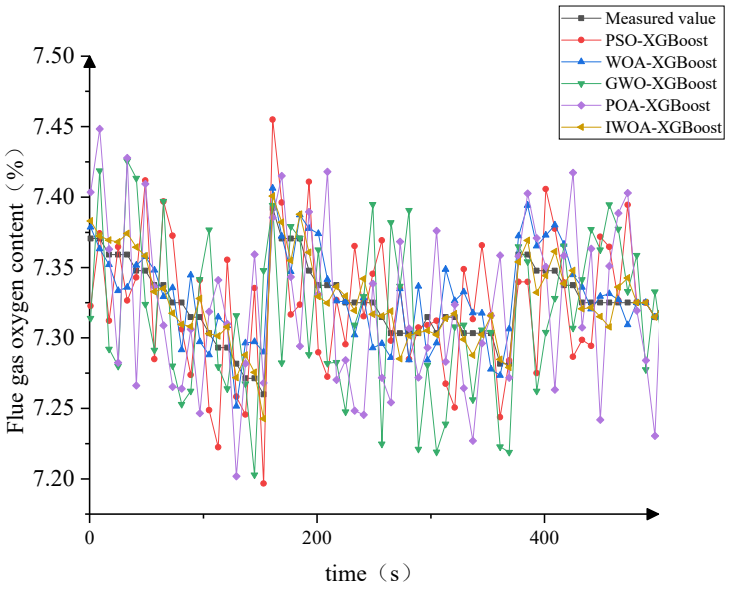


Figure 12. Comparison of forecast results among different models.

Another example is at 300 s. The PSO-XGBoost predicted value is about 7.28%, the WOA-XGBoost is about 7.32%, and the IWOA-XGBoost is around 7.36. The measured value at this moment is about 7.37, so the deviation in IWOA-XGBoost is about 0.01%, which is much smaller than the deviations of PSO-XGBoost (about 0.09%) and WOA-XGBoost (about 0.05%).

By calculating the root-mean-square error (RMSE) of each model throughout the time period, the RMSE of PSO-XGBoost is found to be around 0.08, that of WOA-XGBoost is about 0.05, and that of IWOA-XGBoost is only about 0.02. These specific data fully demonstrate that the IWOA-XGBoost model has higher prediction accuracy and is closer to the measured values compared with the WOA-XGBoost and PSO-XGBoost models, thus proving the feasibility and accuracy of the IWOA-XGBoost model in predicting flue gas oxygen content.

To verify the degree to which the established prediction model approximates the real process, the autocorrelation function test method is adopted to test the proposed prediction model. Figure 13 shows the autocorrelation function of the normalized deviation between the flue gas oxygen content calculated by the prediction model proposed in this paper and the measured flue gas oxygen content.

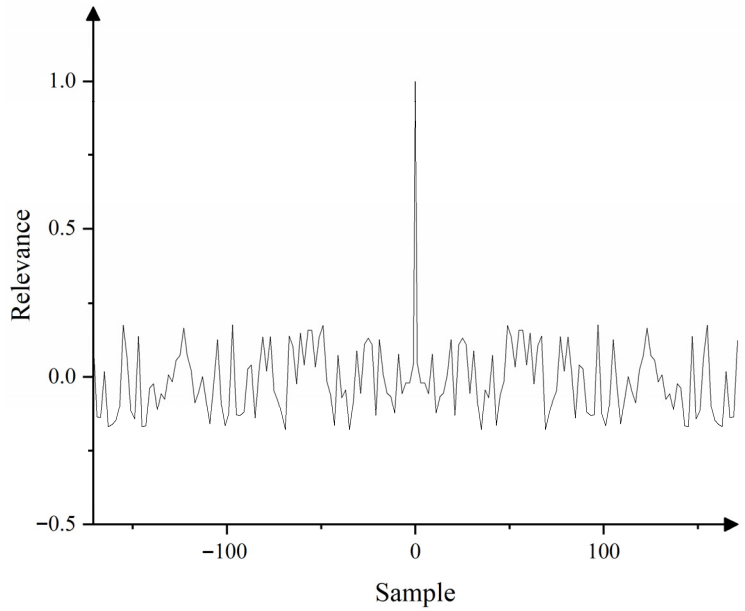


Figure 13. Autocorrelation distribution map of oxygen content deviation in flue gas.

It can be seen from the figure that the autocorrelation coefficients of the deviation sequence between the predicted flue gas oxygen content and the measured flue gas oxygen content basically fall within the confidence interval. Therefore, the residual sequence can be considered a white noise sequence, which further proves that the flue gas oxygen content prediction model is close to the actual process in terms of flue gas oxygen content calculation.

Figures 14 and 15 depict the iterative optimization processes of the proportional (P) and integral (I) parameters for the feedback compensation model and the predictive compensation model of flue gas oxygen content control variables, respectively, using the improved firefly algorithm (IFA).

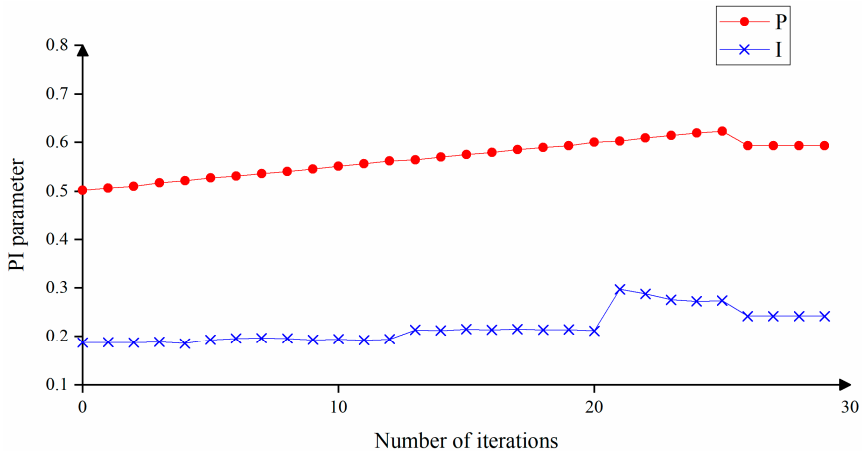


Figure 14. The PI parameter optimization diagram of the feedback compensator.

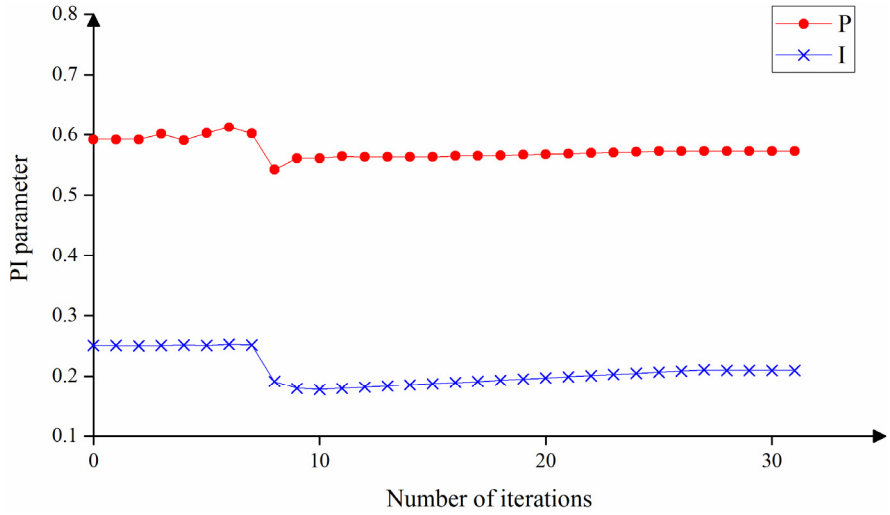


Figure 15. The PI parameter optimization diagram of the forecast compensator.

In Figure 14, for the feedback compensation model: K_{bp} parameter shows a continuous upward trend in the early stage of iteration, gradually stabilizing as the number of iterations increases, finally approaching an optimal value of around 0.515. The K_{bi} parameter initially remains relatively stable but then rises and stabilizes at approximately 0.255 after about 20 iterations. This indicates that IFA effectively searches for the optimal P and I parameter combination for the feedback compensation model, with the curves' variations becoming gradual and stable after 30 iterations, suggesting that the algorithm converges to a global optimal solution for the feedback compensation model's PI parameters.

In Figure 15, for the forecast compensation model, the K_{fp} parameter first rises, then experiences a slight drop before stabilizing at around 0.531. The K_{fi} parameter shows a decreasing trend initially and then stabilizes at about 0.216. Similarly, after 30 iterations, the curve changes stabilize, demonstrating that IFA successfully finds the optimal PI parameter combination for the predictive compensation model as well.

Overall, these two figures illustrate that the IFA can efficiently explore and converge to the optimal P and I parameter combinations for both the feedback and forecast compensation models. After 30 iterations, the parameter curves stabilize, indicating that the algorithm has found the global optimal solutions. The final PI parameter combination for the forecast compensator is $K_{fp} = 0.531$, $K_{fi} = 0.216$ and $K_{bp} = 0.515$, $K_{bi} = 0.255$ for the feedback compensator.

To clarify the effect of the hybrid closed-loop control, this experiment conducted a comparative test on the control of oxygen content in flue gas, as follows:

In this experiment, the flue gas oxygen content prediction model based on IWOA was tested and verified to have a prediction deviation range of ±0.2%.

As can be seen from Figure 16, when only the set control model is adopted and the target value is changed at 700 s, the overshoot of the oxygen content deviating from the target value is greater than 3%, and the adjustment time is greater than 200 s. This indicates that the single-setting control model has limited timeliness and accuracy in deviation correction when dealing with dynamic disturbances, and it is necessary to combine a compensation mechanism to improve the performance of dynamic control.

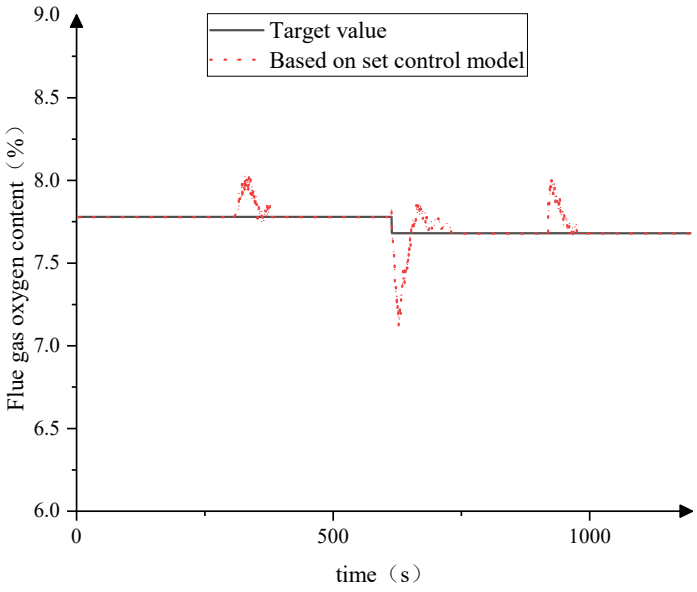


Figure 16. Control effect diagram based on the set control model.

After introducing the forecast compensation based on the forecast model, the experimental results are shown in Figure 17. Except for the deviation at 700 s due to the sudden change in the target value, the range of oxygen content deviation from the target value in other periods was stable within ±0.2%, which was in line with the deviation range of the forecast model.

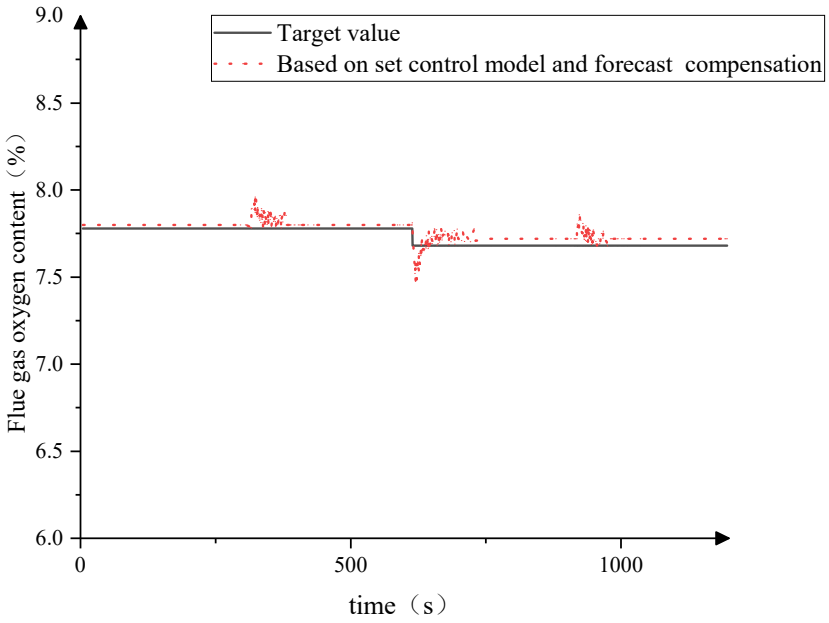


Figure 17. Control effect diagram based on set control model and forecast compensation.

The control effects of three flue gas oxygen content control methods are shown in Figure 18. It can be seen from the figure that under the control of the setting control method proposed in this paper, the flue gas oxygen content stabilizes at 7.78%. The MPC-based flue gas oxygen content control method maintains the flue gas oxygen content at 7.75%. The setting control method used in the solid waste incineration plant controls the flue gas oxygen content at 7.85%.

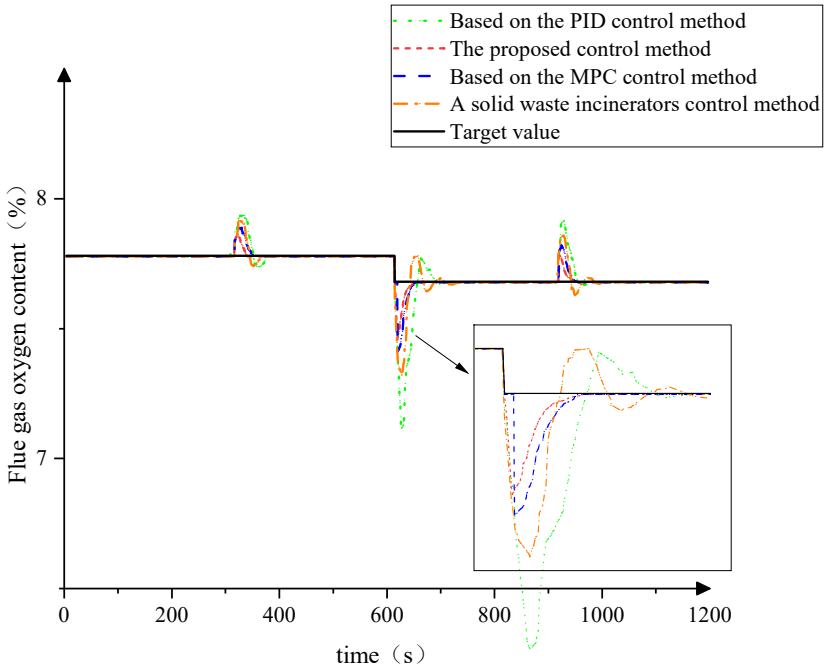


Figure 18. Effect diagram of oxygen content control in flue gas.

The analysis of the above experimental results is presented in Table 5, which analyzes the control performance indicators of the three control methods. For the PID-based control method, the overshoot is 2.73%, the relative error is 1.127%, and the adjustment time is 100 s. The overshoot of the control method proposed in this paper is 1.53%, its relative error is −0.094%, and its system adjustment time is 90 s. For the MPC-based control method, the overshoot is 2.1%, the relative error is −0.529%, and the adjustment time is 150 s. Under the control of the domestic solid waste plant, the overshoot is 2.35%, the relative error is 0.835%, and the adjustment time is 180 s.

Table 5. Analysis of the control performance indicators of three control methods.

Method	Adjust the Time	Amount of Overshoot	Relative Error
The control method of this article	90	1.53%	−0.094%
Based on the MPC method	100	2.1%	−0.529%
Control methods for a certain solid waste incineration plant	140	2.35%	0.835%
Based on the PID control method	150	2.73%	1.127%

It can be seen that although all three control methods can meet the control target, the setting control method proposed in this paper has the smallest overshoot and the shortest adjustment time by comparison. In contrast, the control method of the domestic solid waste plant has the largest overshoot and the longest adjustment time. These results indicate that the hybrid intelligent setting control method for flue gas oxygen content proposed in this paper can quickly control the flue gas oxygen content to reach the control target when operating conditions change. Compared with the other two control methods,

the proposed method can adapt to variable operating conditions with stronger control capability and better anti-interference ability.

Despite its significant control effects, the method has certain limitations. The performance of the control system depends on accurate state measurement and prediction models. However, in some incineration plants in developing countries, sensor accuracy and data collection frequency may not fully meet the requirements. Additionally, factors such as changes in waste composition and fluctuations in moisture content may affect system stability and control effectiveness. In the future, advanced algorithms such as deep learning and reinforcement learning can be introduced to further enhance the system's adaptability and prediction accuracy. Meanwhile, strengthening the integration of multi-source data and intelligent transformation will provide stronger technical support for the optimization and sustainable development of the solid waste incineration process.

5. Conclusions

This study proposed a hybrid intelligent closed-loop control method integrating feedforward and feedback mechanisms for precise regulation of flue gas oxygen content in municipal solid waste incineration (MSWI) systems. By combining modeling and control technologies, the proposed approach effectively distinguishes between measurable and unmeasurable disturbances. The preset manipulated variable model provides a benchmark for control operations, while the feedforward compensation model proactively corrects the primary and secondary air volumes according to measurable disturbances. Simultaneously, the feedback compensation mechanism dynamically adjusts for unmeasurable disturbances based on real-time oxygen deviation, maintaining combustion stability under complex and varying conditions.

Experimental validation using real operational data from a 600 t/d MSWI plant confirmed that the proposed hybrid control method substantially enhances combustion performance. Compared with conventional PID and standalone fuzzy control methods, the proposed system achieved a 34.9% reduction in overshoot, 50% faster response time, and an over 80% improvement in steady-state control accuracy of flue gas oxygen content. These quantitative results demonstrate that integrating the firefly algorithm (FA) and whale optimization algorithm (WOA) enables adaptive parameter optimization in real time, leading to superior robustness, precision, and stability in large-scale waste-to-energy applications.

While the results are promising, the study acknowledges that the effectiveness of the proposed method relies on accurate state measurement and reliable prediction models. In practical scenarios—especially in developing regions where sensor precision and data acquisition frequency may be limited—system performance could be affected. Future work will, therefore, focus on developing calibration and redundancy mechanisms to mitigate sensor-related limitations, and on incorporating multi-source data fusion to enhance the resilience and sustainability of the control system.

Furthermore, future research will focus on exploring deep learning and reinforcement learning techniques to further improve prediction accuracy and system adaptability. By integrating these cutting-edge approaches with intelligent transformation frameworks, the hybrid control strategy can evolve toward a more autonomous, adaptive, and sustainable intelligent control system suitable for real-world industrial environments.

Author Contributions: Methodology, J.P. and Y.Y.; validation, Y.Y.; formal analysis, Y.Y.; resources, J.T.; writing—original draft, J.P.; writing—review and editing, J.T. and J.H. All authors have read and agreed to the published version of the manuscript.

Funding: This research received no external funding.

Data Availability Statement: The original contributions presented in this study are included in the article. Further inquiries can be directed to the corresponding author.

Conflicts of Interest: The authors declare no conflicts of interest.

Abbreviations

The following abbreviations are used in this manuscript:

MSW	Municipal Solid Waste
MSWI	MSW Incineration
ACC	Automation Combustion Control
PID	Proportional–Integral–Derivative
MPC	Model Predictive Control
WOA	Whale Optimization Algorithm
IWOA	Improved Whale Optimization Algorithm
XGBoost	eXtreme Gradient Boosting
FA	Firefly Algorithm
IFA	Improved Firefly Algorithm
PI	Proportional–Integral
$\dot{m}_{O_2}$	Consume oxygen mass flow per unit time
$\dot{m}_{fuel}$	Mass flow rate of refuse entering furnace per unit time
a	Fuel stoichiometry (molar ratio of oxygen to organic matter)
M_{fuel}	Molecular weight of fuel consumed through mass balance and oxygen
u_1	Input the air flow rate once
u_2	Input the secondary air flow rate
Ω_1	Input the working conditions and feeding speed
Ω_2	Input the working condition and grate speed
$y(t)$	Oxygen content in flue gas
O^*	Ideal oxygen content target value
$\hat{y}(t)$	Forecast value of oxygen content in flue gas
U_0	Benchmark operation volume
$e_f(t)$	Forecast compensation deviation
$U_f(t)$	Forecast compensation value
$U_b(t)$	Feedback compensation value
$e_b(t)$	Feedback compensation deviation
S	Stable Interval
ε	The maximum tolerated deviation
τ_d	Time constant
D	Maximum decision tree depth
λ	Learning rate
φ	Regularization coefficient
T	Leaf nodes
w_j	Leaf weights
t	Current number of iterations
$X(t)$	Position vector of the current search candidate solution
$X^*(t)$	Position vector of the current optimal search candidate solution
A	Coefficient matrix
C	Coefficient matrix
r_1	Random vector
r_2	Random vector
b	Constants that determine the shape of the spiral path
$X_{rand}(t)$	Randomly search for the position vectors of candidate solutions
$\widetilde{w}_{i,j}$	Reconstruct the j-dimensional vector of solution w_i

$lb_j = \min(w_{i,j})$	The boundary of the population space
$ub_j = \min(w_{i,j})$	The boundary of the population space
p	Probability value
v	Degree of freedom
$\Gamma(\bullet)$	gamma function
max_*iteration*	Maximum number of iterations
N	Sample size
x_{best}	The current best whale
FA_i	Position of each firefly i
$\mu_k^{(i)}$	Range of parameters that need to be constrained
I_i	Brightness
β	The greatest attraction
β_0	The attraction of fireflies at the light source ($\gamma = 0$)
γ	Light intensity absorption coefficient
γ_{ij}	Euclidean distance between fireflies
θ	Random step size factor
ε_i	Random perturbation vector
$\omega(t) \times x_j(t)$	The influence of the previous iteration position of a firefly individual on its current position
$\omega(t) \times rand \times (x_{best}(t) - x_j(t))$	The traction effect provided by the optimal individual of the current iteration population on the individuals within the population
$f(x_{best}(t))$	The global optimal value of the TTH iteration
$f_i(t-1)$	The value of the $t-1$-th iteration of Firefly i
$f_i(t-2)$	The value of the $t-2$-th iteration of Firefly i
$M(f) = \frac{1}{n}\sum_{i=1}^{n} f(x_i(t))$	The average value of the population objective function in the t-th iteration
σ	The variance of the Gaussian distribution
μ	Expectation
K_{bp}	Proportional gain
K_{bi}	Integral time constant
K_{fp}	Proportional gain
K_{fi}	Integral time constant

References

1. Khan, S.; Anjum, R.; Raza, S.T.; Bazai, N.A.; Ihtisham, M. Technologies for municipal solid waste management: Current status, challenges, and future perspectives. *Chemosphere* **2022**, *288*, 132403. [CrossRef] [PubMed]
2. Cui, Y.; Meng, X.; Qiao, J. Dynamic sequential transfer optimization for municipal solid waste incineration process under multiple operating conditions. *Eng. Appl. Artif. Intell.* **2025**, *195*, 111519. [CrossRef]
3. Guo, J.; Dong, Z.; Guo, W.; Yan, A. Robust stochastic configuration network based perception model for furnace temperature in municipal solid waste incineration process. *Inf. Sci.* **2025**, *719*, 122477. [CrossRef]
4. Herceg, S.; Andrijić, Ž.U.; Bolf, N. Support Vector Machine-Based Soft Sensors in the Isomerisation Process. *Chem. Biochem. Eng. Q.* **2025**, *34*, 1825. [CrossRef]
5. Qin, Y.F.; Bai, Y. Modeling and Simulation of Combustion Process of MSW Volatile. *J. Chin. Soc. Power Eng.* **2010**, *30*, 444–449+455.
6. Beylot, A.; Hochar, A.; Michel, P.; Descat, M.; Ménard, Y.; Villeneuve, J. Municipal Solid Waste Incineration in France: An Overview of Air Pollution Control Techniques, Emissions, and Energy Efficiency. *J. Ind. Ecol.* **2018**, *22*, 1016–1026. [CrossRef]
7. Chai, T.; Zhou, Z.; Cheng, S.; Jia, Y.; Song, Y. Industrial Metaverse-Based Intelligent PID Optimal Tuning System for Complex Industrial Processes. *IEEE Trans. Cybern.* **2024**, *54*, 6458–6470. [CrossRef] [PubMed]
8. Lu, J.W.; Zhang, S.; Hai, J.; Lei, M. Status and perspectives of municipal solid waste incineration in China: A comparison with developed regions. *Waste Manag.* **2017**, *69*, 170–186. [CrossRef]

9. Chai, T. Industrial process control systems: Research status and development direction. *Sci. Sin. Informationis* **2016**, *46*, 1003–1015. [CrossRef]
10. Chang, N.B.; Chen, W.C. Fuzzy controller design for municipal incinerators with the aid of genetic algorithms and genetic programming techniques. *Waste Manag. Res.* **2000**, *18*, 429–443. [CrossRef]
11. Shen, K.; Lu, J.D.; Li, Z.; Liu, G. An adaptive fuzzy approach for the incineration temperature control process. *Fuel* **2005**, *84*, 1144–1150. [CrossRef]
12. Ding, H.X.; Tang, J.; Qiao, J. Data-driven Modeling and Self-organizing Control of Municipal Solid Waste Incineration Process. *Acta Autom. Sin.* **2023**, *49*, 550–566. [CrossRef]
13. Tao, J.; Li, Z.; Chen, C.; Liang, R.; Wu, S.; Lin, F.; Cheng, Z.; Yan, B.; Chen, G. Intelligent technologies powering clean incineration of municipal solid waste: A system review. *Sci. Total Environ.* **2024**, *935*, 173082. [CrossRef]
14. Tang, J.; Tian, H.; Wang, T. A Review of Model Predictive Control for the Municipal Solid Waste Incineration Process. *Sustainability* **2024**, *16*, 7650. [CrossRef]
15. Leskens, M.; van Kessel, L.B.M.; Bosgra, O. Model predictive control as a tool for improving the process operation of MSW combustion plants. *Waste Manag.* **2005**, *25*, 788–798. [CrossRef] [PubMed]
16. Fiedler, F.; Karg, B.; Lüken, L.; Brandner, D.; Heinlein, M.; Brabender, F.; Lucia, S. do-mpc: Towards FAIR nonlinear and robust model predictive control. *Control. Eng. Pract.* **2023**, *140*, 105676. [CrossRef]
17. Yan, A.; Wang, R.; Guo, J.; Tang, J. A knowledge transfer online stochastic configuration network-based prediction model for furnace temperature in a municipal solid waste incineration process. *Expert Syst. Appl.* **2024**, *243*, 122733. [CrossRef]
18. Nguyen, T.D.; Kawai, K.; Nakakubo, T. Drivers and constraints of waste-to-energy incineration for sustainable municipal solid waste management in developing countries. *J. Mater. Cycles Waste Manag.* **2021**, *23*, 1688–1697. [CrossRef]
19. Afram, A.; Janabi-Sharifi, F. Theory and applications of HVAC control systems—A review of model predictive control (MPC). *Build. Environ.* **2014**, *72*, 343–355. [CrossRef]
20. Sun, J.; Meng, X.; Qiao, J. Data-Driven Optimal Control for Municipal Solid Waste Incineration Process. *IEEE Trans. Ind. Inform.* **2023**, *19*, 11444–11454. [CrossRef]
21. Wen, C.; Lin, X.; Ying, Y.; Ma, Y.; Yu, H.; Li, X.; Yan, J. Dioxin emission prediction from a full-scale municipal solid waste incinerator: Deep learning model in time-series input. *Waste Manag.* **2023**, *170*, 93–102. [CrossRef]
22. Tang, J.; Wang, T.; Xia, H.; Cui, C. An Overview of Artificial Intelligence Application for Optimal Control of Municipal Solid Waste Incineration Process. *Sustainability* **2024**, *16*, 2042. [CrossRef]
23. Tian, H.; Tang, J.; Wang, T. Furnace Temperature Model Predictive Control Based on Particle Swarm Rolling Optimization for Municipal Solid Waste Incineration. *Sustainability* **2024**, *16*, 7670. [CrossRef]
24. Fan, Y.; Liu, X.; Zhang, C.; Li, C.; Li, X.; Wang, H. Dynamic Prediction of Boiler NOx Emission with Graph Convolutional Gated Recurrent Unit Model Optimized by Genetic Algorithm. *Energy* **2024**, *294*, 130957. [CrossRef]
25. Aslam, M.U.; Shakhawat, N.S.B.; Shah, R.; Amjady, N.; Miah, S.; Amin, B.M.R. Hybrid Energy Storage Modeling and Control for Power System Operation Studies: A Survey. *Energies* **2024**, *17*, 5976. [CrossRef]
26. He, H.J.; Meng, X.; Tang, J.; Qiao, J. Research on Modeling and Control of Furnace Temperature for Municipal Solid Waste Incineration Process. *Control. Eng. China* **2023**, *30*, 1852–1862. [CrossRef]
27. Thai, S.M.; Wilcox, S.J.; Chong, A.Z.S.; Ward, J. Combustion optimisation of stoker fired boiler plant by neural networks. *J. Energy Inst.* **2008**, *81*, 171–176. [CrossRef]
28. Caetano, N.R. Review on the Theoretical and Practical Applications of Symmetry in Thermal Sciences, Fluid Dynamics, and Energy. *Symmetry* **2025**, *17*, 1240. [CrossRef]
29. Wan, X.; Li, Y.; Wang, Y.; Li, Y.; Zhang, C. Recent Advances in Chiral and Achiral Metasurfaces Under Symmetry Preservation and Breaking. *Symmetry* **2025**, *17*, 1001. [CrossRef]
30. Chai, T.; Zheng, R.; Xing, F.; Jia, Y.; Zheng, X. Intelligence for Industrial Process Control: Development and Prospects. *Sci. Sin. Informationis* **2025**, *55*, 1555. [CrossRef]
31. Pian, J.; Liu, J.; Tang, J.; Hou, J. Intelligent Control of the Main Steam Flow Rate for the Municipal Solid Waste Incineration Process. *Sustainability* **2025**, *17*, 6036. [CrossRef]
32. Bai, J.Y.; Bai, Z.G. Study on Automaticstrategy for Chain Grate in Msw Incinarator. *Therm. Power Gener.* **2008**, *37*, 109–113. [CrossRef]
33. Long, J.S.; Yang, W.Y.; Zhang, H.Y. Research on the Influence of Automatic Combustion Control System on Main Parameters of Boiler Operation in a Waste Incineration Plant. *Environ. Sanit. Eng.* **2023**, *31*, 49–54. [CrossRef]
34. Sun, J.; Meng, X. Adaptive Predictive Control of Oxygen Content in Flue Gas for Municipal Solid Waste Incineration Process. *Acta Autom. Sin.* **2023**, *49*, 2338–2349. [CrossRef]
35. Fu, Z.; Zou, H. Soot Blowing Scheme Optimization for Small Scale Circulating Fluidized Bed Boilers Using XGBoost. *Control. Eng. China* **2025**, *32*, 891–896. [CrossRef]

36. Liang, W.; Xue, W. Soft Measurement of Main Steam Flow in Municipal Solid Waste Incinerator Based on WOA-Elman Neural Network. *Control. Eng. China* **2025**, *32*, 201–207. [CrossRef]
37. Wang, H.J.; Zhang, L. Whale Optimization Algorithm Based on Chaotic Search Strategy. *Control. Decis.* **2019**, *34*, 1893–1900. [CrossRef]
38. Tian, M.C.; Bo, Y.M.; Chen, Z.M.; Wu, P.L.; Zhao, G.P. Firefly Algorithm Intelligence Optimized Particle Filter. *Acta Autom. Sin.* **2016**, *42*, 89–97. [CrossRef]
39. Liu, C.Y.; Ren, Y.Y. Timing Optimization of Regional Traffic Signals Based on Improved Firefly Algorithm. *Control. Decis.* **2020**, *35*, 2829–2834. [CrossRef]

Disclaimer/Publisher's Note: The statements, opinions and data contained in all publications are solely those of the individual author(s) and contributor(s) and not of MDPI and/or the editor(s). MDPI and/or the editor(s) disclaim responsibility for any injury to people or property resulting from any ideas, methods, instructions or products referred to in the content.